Relativistic many-body methodology of electric dipole oscillator strengths with application to Tl^+ $6s^2 \rightarrow 6s6p$

Donald R. Beck and Ziyong Cai
Department of Physics, Michigan Technological University, Houghton, Michigan 49931
(Received 16 May 1988; revised manuscript received 10 August 1989)

A systematic way of simultaneously handling relativistic and many-body effects for electric dipole transition probabilities is introduced. Relativistic many-body wave functions are generated using a relativistic configuration-interaction (RCI) approach, where the virtual space is represented by screened hydrogenic functions whose effective charges are determined during the RCI process. It is shown that the number of "parents" that must be kept in a first-order wave function may be minimized, using a procedure called REDUCE. The relativistic form of the first-order theory of oscillator strengths is used to determine which configurations are crucial. Application is made to the Tl^+ $6s^2 \rightarrow 6s6p\ ^{1,3}P_1$ transitions for which both nonorthonormality and core excitation effects are found to be crucial. For the allowed transition, our results (length and velocity) are in excellent agreement with experiment.

I. INTRODUCTION

This article is the fourth in a series[1-3] whereby our nonrelativistic many-body wave function[4,5] and property[6-8] theory and computer algorithms are being replaced with their fully relativistic analogs. Our motive for doing this is twofold: (i) once the work is complete, we will be able to accurately calculate lifetimes of excited states of first-row transition-metal negative ions (having such lifetimes will enable one to predict whether the state is truly bound or "merely" a resonance); (ii) there does not exist a comprehensive relativistic many-body methodology to date, and this makes treatment of more than half of the atoms in the Periodic Table difficult.

In this work, we report the completion of a fully relativistic configuration-interaction (CI) approach from which the wave functions will be generated. There are two major novel features present in our RCI work.

(i) The way in which the radial parts of the virtual spinors are created. Since we wish to use basis functions (as opposed to numerical solutions of differential equations), we run the risk of variational collapse[9] into the "position sea." Recent work by others,[10] at the zeroth-order level, suggests that resolution of this problem lies in using appropriately balanced major and minor basis sets. We have achieved this condition by representing our virtual basis sets by screened hydrogenic functions, for which a single energy-optimized parameter (effective charge) serves to specify both major and minor components.

(ii) We introduce a relativistic version of our REDUCE procedure,[1] which minimizes the number of "parents" that have a nonzero interaction with the zeroth-order solution. In a first-order many-body wave function, those with zero interaction can be discarded.

Next, we present details of the theory and computational algorithms which take the RCI wave functions, and evaluate the electric dipole transition probability. Our procedure uses both the length and velocity gauges, fully accounts for nonorthonormality, and includes a prescription, the first-order theory of oscillator strengths[11] (FOTOS), which identifies the most important configurations which must be included in RCI wave functions to obtain accurate results.

A "flow diagram" for the entire procedure is shown in Fig. 1. In Sec. II we discuss the RCI formalism, in Sec. III the oscillator-strength formalism, and in Sec. IV the results of applying the formalism to the Tl^+ $6s^2 \rightarrow 6s6p$ transitions.

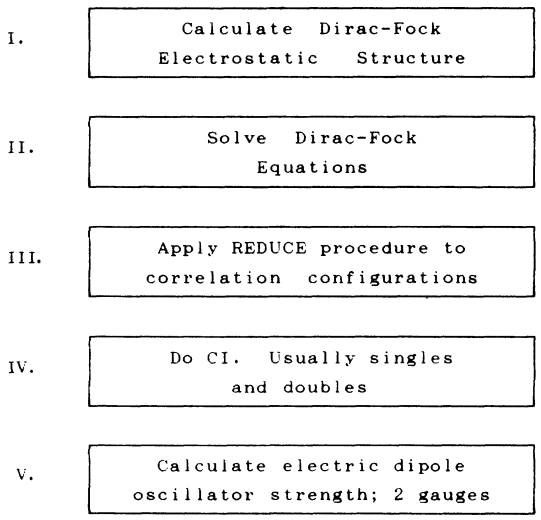

FIG. 1. Relativistic "flow chart."

II. THE RCI FORMALISM

A. Relativistic CI theory

The Hamiltonian is given by (in a.u.)

$$H_{\rm rel}=\sum_{i=1}^{N}[c\boldsymbol{\alpha}_i\cdot\mathbf{p}_i+\beta_i c^2+V_N(r_i)]+\sum_{\substack{i,j\\(i<j)}}r_{ij}^{-1}+\sum_{\substack{i,j\\(i<j)}}\left[\frac{-\boldsymbol{\alpha}_i\cdot\boldsymbol{\alpha}_j}{r_{ij}}+\frac{(\boldsymbol{\alpha}_i\cdot\mathbf{p}_i)(\boldsymbol{\alpha}_j\cdot\mathbf{p}_j)}{2}r_{ij}\right],$$

where the one-body operators form the Dirac Hamiltonian [$V_N(r)$ can represent either the point nucleus or a finite spherical nuclear charge distribution], and the last two operators are the magnetic and retardation parts of the Breit operator.

As a zeroth-order function, we use a multiconfigurational Dirac-Fock (MCDF) solution, obtained from a modified[2,3] form of Desclaux's[12] program. Normally, all configurations which arise from a single nonrelativistic configuration will constitute the MCDF solution (e.g., for $6s6p$ we use $6s_{1/2}6p_{1/2}$ and $6s_{1/2}6p_{3/2}$).

Now the perturbation $V=H-H_0$, where H_0 is the multiconfigurational Dirac-Fock Hamiltonian, is a sum of two electron operators only, and is composed of a portion of the Coulomb repulsion and, normally, the complete Breit operator (we allow the option of having the Breit operator in the MCDF matrix, but it does not appear explicitly in the MCDF differential equations). For most applications the residual Coulomb repulsions will dominate the perturbation, thus allowing us to invoke our nonrelativistic experience as to what configurations to include in the RCI wave functions.

In particular, generalizing from this experience, the following five types of configurations will be found in a first-order wave function (i.e., one whose configurations are chosen using first-order perturbation theory):

(i) $n_1l_1j_1\rightarrow n_2l_2j_2$, $(-1)^{l_1}=(-1)^{l_2}$;

(ii) $nl_1j_1\rightarrow vl_2j_2$, $(-1)^{l_1}=(-1)^{l_2}$;

(iii) $n_1l_1j_1, n_2l_2j_2\rightarrow n_3l_3j_3, n_4l_4j_4$, $(-1)^{l_1+l_2}=(-1)^{l_3+l_4}$;

(iv) $n_1l_1j_1, n_2l_2j_2\rightarrow n_3l_3j_3, vl_4j_4$, $(-1)^{l_1+l_2}=(-1)^{l_3+l_4}$;

(v) $n_1l_1j_1, n_2l_2j_2\rightarrow v_1l_3j_3, v_2l_4j_4$, $(-1)^{l_1+l_2}=(-1)^{l_3+l_4}$;

for (iii)–(v) the ranges $|j_1-j_2|,j_1+j_2$ and $|j_3-j_4|,j_3+j_4$ must overlap; the same condition also applies for the orbital angular momentum.

To illustrate the notation, (iv) means two spinors from subshells $n_1l_1j_1$ and $n_2l_2j_2$ are removed from the MCDF configuration [steps (i)–(v) must be carried out for every configuration present in the zeroth-order function] and replaced by spinors from subshells $n_3l_3j_3$ and vl_4j_4 (the former is a subshell present in the MCDF solution, but not fully occupied in the current MCDF configuration, and vl_4j_4 is a virtual subshell—unoccupied in any MCDF configuration).

It is perhaps easier to create the configurations nonrelativistically, and then convert them to their relativistic form. Consider $5d^{10}\,6s6p$ ($J=1$); a contribution of type (iv) is $5d6p\rightarrow 6svf$, yielding $5d^96s^2vf$. In relativistic form (specifying only the open subshells), we have $6s_{1/2}6p_{1/2}$ and $6s_{1/2}6p_{3/2}$ as the MCDF configurations, being correlated with $5d_{3/2}^{-1}vf_{5/2}$, $5d_{5/2}^{-1}vf_{5/2}$, and $5d_{5/2}^{-1}vf_{7/2}$. The notation $5d_j^{-1}$ tells us which $5d$ subshell is missing an electron, i.e., it identifies the hole.

The many-body wave function is expanded in terms of configurational eigenstates of J^2, J_z, and parity [similar restrictions can be made on groups of electrons; the electrons may also be coupled to form approximate eigenstates of L^2 and S^2, if desired (details are given in Ref. 2)].

B. The REDUCE method

In many cases, there will be many angular eigenstates (parents) connected with each nonrelativistic configuration. For example, if $3d^6$ is coupled to $J=0$, and we wish to correlate this with $3d^4vd^2$ ($J=0$), there are 58 relativistic eigenstates having $J=0$ (for the nonrelativistic case, there are 2 for $^7F_0$, 17 for $^5D_0$, 29 for $^3P_0$, and 10 for $^1S_0$, so we have at most 29 to deal with; here we are helped by the fact that L and S are good quantum numbers). Retaining all these relativistic eigenstates would present us with significant computational expenses in setting up and diagonalizing the energy matrix. To avoid this, we introduce the relativistic form of the REDUCE method.[1] Considering only the Coulomb repulsion's contribution to the perturbation, we find that all matrix elements,

$$\left\langle 3d^6(J=0)\left|\sum_{i,j}r_{ij}^{-1}\right|3d^4vd^2(J=0)\right\rangle ,$$

can be expressed as a linear combination of 19 relativistic radial integrals (all relativistic configurations "resulting from" the same nonrelativistic configuration must be treated as a unit—both in the MCDF function and for the correlation configuration). The two electron electrostatic radial integrals R^k $(3d_j3d_{j'};vd_{\bar{j}}vd_{\bar{j}'})$ appear with the following combinations:

$$(k;2j;2j';2\bar{j};2\bar{j}')=(0,2;3;3;3;3),\ (2;3;3;3;5),\ (2,4;3;3;5;5),\ (2;3;5;3;3),\ (0,2;3;5;3;5),$$
$$(2,4;3;5;5;3),\ (2,4;3;5;5;5),\ (2,4;5;5;3;3),\ (2,4;5;5;3;5),\ (0,2,4;5;5;5;5),$$

where we have made use of permutation symmetry to require $j\le j'$, and if $j=j'$, $\bar{j}\le\bar{j}'$. This means that we can rotate (linearly transform) the 58 eigenstates (or parents) to a form where $58-19=39$ of the new parents have a zero matrix element with the MCDF wave function, and can be discarded if a first-order RCI wave function is desired. Furthermore, if the problem is substantially nonrelativistic, there would only be three unique,

nonzero, radial integrals, and a further 16 parents could be discarded. These electrostatic radial integrals are of the direct type; they are $F^0(3d,vd)$, $F^2(3d,vd)$, and $F^4(3d,vd)$. In the absence of j-dependent radial functions, the 19 relativistic radial integrals listed above collapse to these three. One can obviously split the surviving 19 into two groups (16+3), and allow the calculation itself to determine if any of the 16 survive. These ideas have just been automated (program RELRED) by one of us.[13]

Of course, problems will arise where the contribution of the Breit operator will force us to retain parents not surviving electrostatically. If there were N radial Breit integrals, then $19+N$ parents would survive.

C. Virtual basis sets

Prior to the mid-1960s, nonrelativistic CI treatments of many electron effects were represented by configurations whose virtual basis sets were drawn from "optical" configurations in the case of numerical methods, or, in the case of basis-set methods, from the unoccupied orbitals produced during the matrix Hartree-Fock solution process.

In the late 1960s two closely related efficient methods were developed,[14,15] both of which recognized that because correlation was a localized phenomena in first-order perturbation theory, it might be possible to replace an entire Rydberg series with only a few well-chosen localized configurations. For a simple case, namely, the ground state of Be, viz., $1s^22s^2$, the methods developed were able to replace the entire Rdyberg series $1s^22s$ $(3s+4s+5s+\cdots+\epsilon s)$ with very few new configurations $1s^22s$ $(vs+vs'+\cdots)$, for which the virtual basis sets were quite well localized (having an average r near that of the $2s$ orbital).

While both methods chose the same form (preorthogonalization) for the virtual basis sets, that of Slater-type orbitals (STO's), which are portions of screened hydrogenic functions, they differed in how the nonlinear parameter (negative exponent) was to be chosen. In one method,[14] the energy variational principle (via minimization of the CI matrix) was employed; in the other,[15] an even-tempered virtual STO set was generated. The question of how many STO's it took to represent a single Rydberg series was, to a considerable extent, quickly solved. Computational experience showed that one well-optimized STO was able to "capture" about 70% of the correlation energy for a single series, and that two captured about 90% of the energy. Convergence was slow after this, however; often up to six STO's are required[16] to match experimental accuracies for total energies of small systems. All have negative exponents characteristic of bound functions. It is worth noting that this last work[16] demonstrated that a one-particle basis could indeed be used to generate results of spectroscopic accuracy; e.g., a Hylleraas-type basis set, which can only be employed for very small atoms at the present time, was not necessary. Similar accuracies were achieved for oscillator strengths. These matters are reviewed in further detail in Refs. 5 and 6, and in the references therein.

Although we argued earlier in this work that many-body effects for relativistic atoms were likely to be dominated by the nonrelativistic electrostatic operator, it was noted sometime ago in relativistic matrix Hartree-Fock treatments[10] of atoms and molecules that variational collapse may occur, to the extent that computed total energies may be actually below experimental total energies. Since the many-body methods we wish to employ represent virtual basis sets in terms of basis-set elements (STO's, nonrelativistically), it behooves us to tread with some care in putting forth a method for generating virtual basis sets in a relativistic context.

Recent work on this problem by others[10] at the Dirac-Fock level suggests that the main problem (which arises for the $c\boldsymbol{\alpha}\cdot\mathbf{p}$ operator, and so can hardly be avoided in any context) lies in the failure to provide balanced major- and minor-component basis sets. That is to say, if one chooses a major-component basis set, one is then not free to independently choose a set for the minor component. Some authors[10] provide a prescription for generating the minor-component set; one choice is to let $\boldsymbol{\alpha}\cdot\mathbf{p}$ operate on each major-component basis-set element to generate all elements of the minor-component set.

In this work, we put forward a related but somewhat different idea. We wish to still be able to optimize each virtual basis set by minimizing the CI energy, but in a way that couples both the major and minor components so as to eliminate any variational-collapse problems. The simplest virtual form that comes to mind that might do this is a relativistic hydrogenic-type function whose effective charge would be a nonlinear parameter determined during the CI step. This is also as close as we can get to the nonrelativistic virtual form, that of a STO, which is a portion of a nonrelativistic hydrogenic function. It is important to note that screening constants bear little resemblance to the nuclear charge Z. They may in fact exceed Z. Estimates for these quantities can be obtained[5,6] by choosing the effective charge such that the virtual has an average r identical to that of the occupied function it is replacing. With these comments, it can be appreciated that the unoccupied solutions obtained during the matrix Hartree-Fock process, or the "extra" functions that can be generated from numerical Hartree-Fock methods, bear little resemblance to the virtual basis sets discussed here. In fact, it has long been known that such functions characterize an $(N+1)$-electron system (and are consequently too diffuse), rather than the N-electron system of interest to us.

To test for possible variational collapse, we examined the following cases using variationally optimized screened relativistic hydrogenic virtual basis sets.

(i) Several atoms in the He $1s^2$ isoelectronic sequence ($Z=2,10,80$) were correlated with the results shown in Table I. In the relativistic CI calculations ("Rel. CI" row in Table I), the virtual functions (two for each of the symmetries $s_{1/2}$, $p_{1/2}$, $p_{3/2}$, $d_{3/2}$, $d_{5/2}$, $f_{5/2}$, and $f_{7/2}$ for $Z=2,10$, and one of each for $Z=80$) were represented by optimized (during the CI process) screened hydrogenic functions. Analogous nonrelativistic CI calculations were then made using our nonrelativistic CI program; i.e., two optimized virtual STO's were used for s, p, d,

TABLE I. Total energy for the He $1s^2$ isoelectronic sequence.

Contribution		$Z=2$	$Z=10$	$Z=80$
Relativistic CI	DF[a]	−2.861 813 348	−93.982 767 744	−7002.480 308 41
	Rel. CI[b]	−2.902 223 312	−94.025 748 378	−7002.515 925 4
	Corr.[c]	1.10	1.17	0.969
Nonrelativistic CI	RHF[d]	−2.861 680 00	−93.861 113 55	−6350.111 013 5
	CI[e]	−2.902 228 987	−93.904 255 884	−6350.149 502 08
	Corr.[c]	1.10	1.17	1.05
	Error[f]	46	69	
	CI+Pauli[g]	−2.902 346 302	−94.020 095 884	
Hylleraas[h]	Total (nonrelativistic)	−2.903 724 352	−93.906 806 48	
	Total+Pauli[i]	−2.903 838 678	−94.022 606 48	
	Total+all corrections[j]	−2.903 784 796	−94.008 882 53	
Experiment[k]		−2.903 783 559	−94.008 348 18	
Conversion factor[l]		219 444.534	219 468.594	

[a]Dirac-Fock result, uniform nucleus, in a.u. No Breit contributions.
[b]Total relativistic CI energy, in a.u. No Breit contributions.
[c]Total relativistic correlation energy (=a−b), in eV.
[d]Nonrelativistic Hartree-Fock, in a.u.
[e]Nonrelativistic CI energy obtained from program SMART-PSI [D. R. Beck (unpublished)].
[f]Difference between Hylleraas and e, in meV.
[g]Expectation of one-body, low-Z Pauli operators plus e, in a.u.
[h]C. L. Pekeris, Phys. Rev. **112**, 1649 (1958).
[i]Expectation value of one-body, low-Z Pauli operators.
[j]Orbit-orbit, mass polarization, two-body Darwin, and Lamb-shift corrections added (from h).
[k]From S. Bashkin and J. O. Stoner, Jr., *Atomic Energy Levels and Grotrian Diagrams* (North-Holland, New York, 1975), Vol. I.
[l]The unit is cm^{-1} per a.u.

and f symmetries for $Z=2,10$, and one STO for $Z=80$. The nonrelativistic wave functions were also used (17) to evaluate the expectation value of the one-body low-Z Pauli mass variation with velocity and Darwin operators ("Pauli" row in Table I). To provide a "benchmark," Table I also contains the nonrelativistic results of Pekeris for $Z=2,10$ obtained using Hylleraas methods. The expectation value of the same low-Z Pauli operators were evaluated using Pekeris-Hylleraas wave functions as well.

The calculations have been chosen to make the most careful and "cleanest" comparisons possible. Specifically, the CI results and the Hylleraas results (except for the last entry) are all computed using the nonrelativistic Hamiltonian, and relativistic effects are evaluated using a one-body relativistic Hamiltonian. We next fully corrected (adding two-body relativistic effects, Lamb shift, and mass polarization) the Hylleraas results to allow direct comparison with experiment.

We expect the nonrelativistic results [CI and Hylleraas ("Total+Pauli" rows in Table I)] to differ from one another because of the more incomplete basis (both one electron and N electrons, although errors in the former will dominate) used in the nonrelativistic CI calculations. We can see from Table I that there is a 46-meV error for He $1s^2$ and a 69-meV error for Ne^{8+} $1s^2$ owing to this. Second, it can be seen that the one-body, low-Z Pauli contributions are virtually identical for the two.

How should the relativistic CI results differ from these? Differences can arise from at least six factors.

(1) A different degree of incompleteness of the one- and N-electron bases used to calculate the correlation effects.

(2) The failure of the low-Z Pauli approximation to represent the relativistic Hamiltonian. We may estimate these to be approximately $(Z\alpha)^2$ of the low-Z Pauli contribution.

(3) Changes in the wave function due to relativity.

(4) Different standards of self-consistency imposed at the DF or restricted Hartree-Fock (RHF) levels.

(5) Different nuclear models. The relativistic calculations used a finite nucleus (uniform charge distribution), and the nonrelativistic calculations used a point nucleus.

(6) Contribution of many-body effects to the expectation value of the Breit operator.

Comparison of the relativistic and nonrelativistic CI results shows that for He the relativistic CI result ("Rel. CI" row in Table I) is about 3.3 meV higher, and for Ne, 154 meV lower. In the case of He, most (about 3.8 meV) of the discrepancy originates from the correlation differences, which, however, are only 0.3% of the total correlation energy. In Ne^{8+}, on the other hand, the discrepancy occurs at the DF or RHF+Pauli level. The argument above suggests corrections to the Hamiltonian are an order of magnitude too small to account for the difference. Furthermore, use of a finite nucleus rather than a point-nuclear model contributes only 0.8 meV. The difference is in fact due to a change in the wave func-

tion: If we examine the electrostatic integral $F^0(1s,1s)$, we find it changes from 6.027 657 6 to 6.038 965 4 a.u., the second value being the relativistic one. Since the operator $(1/r_{12})$ is the same in both cases, the difference is due to the change in wave function.

A final comparison can be made with experiment, once the remaining important corrections are added to the Hylleraas one-body, low-Z Pauli result ("Total+Pauli" entry in Table I). The effects which are added are due to mass polarization, two-body low-Z Pauli operators (Darwin, contact spin-spin, and orbit-orbit), and the Lamb shift. Table I shows that when these are present the results ("Total+all contributions") are in good agreement with the experiment: for He, the discrepancy is below 1 cm^{-1} and for Ne it is 117 cm^{-1}. The bulk of the error for Ne (119 cm^{-1}) arises for the prediction of the energy of ^{20}Ne $1s$, and may be due to a poor value for the Lamb shift (on the other hand, the ionization potential for Ne $1s^2$ agrees within to 1 cm^{-1}).

We can continue our comparison of RCI and Hylleraas ("Total+all contributions") results a little further, and inquire as to the contribution of two-particle relativistic effects treated at the RCI level (not done here). For Ne $1s^2$, the DF magnetic contribution is +0.012 109 689 a.u., and the retardation result is zero, as is appropriate for an orbital approximation. The low-Z Pauli equivalent of the retardation operator is the orbit-orbit contribution, which has a Hylleraas (i.e., many-body) value of −0.000 372 71 a.u. The many-body (Hylleraas) value of the magnetic contribution (two-body Darwin plus contact spin-spin contribution) is 0.005 084 45 a.u., quite different from the independent-particle, DF result. On the other hand, a significant discrepancy, traceable to the expectation value of $\delta(r_{12})$, is not unexpected. In Ne $1s^2$, for example, the many-body result (Hylleraas) is 90.3% of the independent-particle value (computed here).

While the discussion of the last paragraph emphasizes the need for a full many-body treatment of the entire Breit operator, if highly accurate results for total energies are desired, all of the analysis tends to confirm that no variational collapse is occurring, and suggests that nonrelativistic concepts and results, insofar as the correlation energy is concerned, provide a useful guideline as to what may be expected relativistically.

For $Z=80$, the low-Z Pauli approximation breaks down, and there are no exact results with which to compare. Comparison of the relativistic and nonrelativistic CI results (see Table I) shows that the two correlation energies remain quite close, and help confirm the presumption that $1s^2$ correlation energy remains relatively constant throughout the Periodic Table. In the next paragraph, we provide a detailed examination of the $1s^2 \rightarrow p^2$ contribution to the correlation energy, which is the largest contributor.

How should these differ? If the system was nonrelativistic, then the off-diagonal matrix elements would satisfy the relationship

$$\langle 1s^2|r_{12}^{-1}|vp^2\rangle = \tfrac{1}{2}\langle 1s^2|r_{12}^{-1}|vp_{1/2}^2\rangle + \frac{\sqrt{3}}{2}\langle 1s^2|r_{12}^{-1}|vp_{3/2}^2\rangle \ .$$

In fact, we have

$$-15.7276 \simeq \tfrac{1}{2}(-6.244)+\frac{\sqrt{3}}{2}(-14.024) = -15.423 \ ,$$

quite close (it is of interest to note that the RCI coefficient of $vp_{3/2}^2$ is 1.8248 times larger than that of $vp_{1/2}^2$—close to the LS limit of $\sqrt{3}=1.732$).

The first-order denominator, $\langle vp^2|H|vp^2\rangle - \langle 1s^2|H|1s^2\rangle$, has a magnitude about 8% larger for $vp_{3/2}^2$ and 18% smaller for $vp_{1/2}^2$ than the nonrelativistic equivalent, which is mainly due to the different one-body operator used. Our results suggest that not only is the $1s^2$ correlation energy for Hg I still nearly constant with Z ($\sim$1.0–1.2 eV), but also that no sign of variational collapse is evident.

For $Z=2$ and 10, an attempt was also made to generate the virtual basis set directly from the MCDF process, but the program[12] failed. This is not so surprising if we realize that virtual basis sets typically involve antiscreening constants, i.e., $Z_{\text{eff}} > Z$, and they can be quite localized; these characteristics can present significant computational challenges to algorithms, especially for cases involving core correlation.

(ii) In correlating the outer subshells of Tl^+ (this work), it was found there was a very strong relationship between our nonrelativistic results and the relativistic ones. Both coefficients and Z_{eff} for large correlation configurations were quite similar. Of course, some change is expected when the average radius of the subshells being correlated undergoes significant change when treated relativistically versus the nonrelativistic treatment (as happens in Hg I, see Ref. 18). Other indirect evidence suggesting no variational collapse is the good agreement obtained with experiment for the f value (see Sec. IV).

D. Miscellaneous details

The following points should be made.

(i) The algorithms used to evaluate the radial integrals in RCI were taken from the Desclaux[12] program.

(ii) We allow the Breit operator to be either included directly in the RCI matrix, or its contribution may be obtained only after the wave function is obtained (first-order perturbation theory).

(iii) The most pressing future modifications needed in RCI are (a) the need to compare determinants rapidly, and (b) the ability to generate angular-momentum eigenstates involving up to several thousand determinants. We think both needs can be met with simple modification of the nonrelativistic algorithms introduced[19] to solve these problems.

III. CALCULATION OF OSCILLATOR-STRENGTHS

A. Oscillator-strength theory

We follow the work of Grant,[20] correcting and extending it where necessary. As our development mainly follows his, details of the derivation will be omitted.

The relativistic absorption oscillator strength, $f_L(J\to J')$ is given by

$$f_L(J\to J')=\frac{c^2|\langle JJ|T_Q^{(L)}|J'J'\rangle|^2}{\Delta E(2J+1)\begin{pmatrix} J & L & J' \\ -J & Q & J'\end{pmatrix}^2(2L+1)}, \tag{1}$$

with

$$T_Q^{(L)}\equiv\sum_{k=1}^{N} t_Q^{(L)}(k),$$

which is a tensor of rank L and component Q.

Our equation differs from Grant's[20] Eqs. 5.1 and 5.2 in three respects.

(i) It is fully many electron; his is restricted to systems with an odd number of electrons. Our result was obtained using standard[21] angular-momentum theory (Wigner-Eckart theorem).

(ii) It supplies a missing factor of c^2.

(iii) It is correctly labeled (absorption, not emission, form).

In Eq. (1), ΔE is the excitation energy (in a.u.) which we always extract from experiment, ( ) is a $3j$ symbol which imposes the condition $Q=J-J'$, the bra is the many-electron lower state ($M=J$), and the ket is the many-electron upper state ($M'=J'$).

The one-electron tensor $t_Q^{(L)}$ is obtained by expanding the field particle interactions in multipoles (which, conveniently, do not interact). For electric multipoles,

$$\begin{aligned} t_Q^{(L)}(k)=\sqrt{\Delta E/\pi c}\Big\{ & G_L\Big[i^L(2L+1)j_L\left[\frac{\Delta E r_k}{c}\right]C_Q^{(L)}(k) \\ & -i^{L+1}\sqrt{(L+1)(2L+3)}[\alpha^{(1)}C^{(L+1)}(k)]_Q^{(L)}j_{L+1}\left[\frac{\Delta E r_k}{c}\right] \\ & +i^{L-1}\sqrt{L(2L-1)}[\alpha^{(1)}C^{(L-1)}(k)]_Q^{(L)}j_{L-1}\left[\frac{\Delta E r_k}{c}\right]\Big] \\ & -i^{L+1}\sqrt{L(2L+3)}[\alpha^{(1)}C^{(L+1)}(k)]_Q^{(L)}j_{L+1}\left[\frac{\Delta E r_k}{c}\right] \\ & -i^{L-1}\sqrt{(L+1)(2L-1)}[\alpha^{(1)}C^{(L-1)}(k)]_Q^{(L)}j_{L-1}\left[\frac{\Delta E r_k}{c}\right]\Big\}, \end{aligned} \tag{2}$$

which follows from Grant's[20] Eqs. 2.5, 2.8, 2.12, and 2.11. Here G_L is a constant which determines the choice of gauge [$G_L=0$ is the Coulomb gauge (velocity) and $G_L=\sqrt{(L+1)/L}$ is the Babushkin[22] gauge (length)]; j is the spherical Bessel function, and

$$C_Q^{(L)}(k)=\sqrt{4\pi/(2L+1)}Y_{LQ}(\theta_k,\varphi_k)$$

where Y_{LQ} is a spherical harmonic.

The final formula needed is the one-electron matrix element involving two spinors and $t_Q^{(L)}$. This can be obtained from Grant's[20] Eqs. 4.8 and 4.10, once the phase factor in his Eq. 4.8 is corrected. We have

$$\begin{aligned} \langle\alpha|t_Q^{(L)}|\beta\rangle=(-1)^{j_\alpha+j_\beta+L+m_\alpha-1/2}\begin{pmatrix} j_\alpha & L & j_\beta \\ \frac{1}{2} & 0 & -\frac{1}{2}\end{pmatrix} \\ \times\begin{pmatrix} j_\alpha & L & j_\beta \\ -m_\alpha & Q & m_\beta\end{pmatrix}\sqrt{(2j_\alpha+1)(2j_\beta+1)}(\bar{t}^{\,e}+G_L\bar{t}^{\,l}), \end{aligned} \tag{3}$$

$$\bar{t}^{\,e}=i^L\{\sqrt{L/(L+1)}[(\kappa_\alpha-\kappa_\beta)I_{L+1}^{+}+(L+1)I_{L+1}^{-}]-\sqrt{(L+1)/L}\,[(\kappa_\alpha-\kappa_\beta)I_{L-1}^{+}-LI_{L-1}^{-}]\}, \tag{4}$$

$$\bar{t}^{\,l}=i^l[(2L+1)J^{(L)}+(\kappa_\alpha-\kappa_\beta)(I_{L+1}^{+}+I_{L-1}^{+})-LI_{L-1}^{-}+(L+1)I_{L+1}^{-}], \tag{5}$$

where the radial integrals are given by

$$I_L^{\pm}=\int_0^\infty(P_\alpha Q_\beta\pm Q_\alpha P_\beta)j_L\left[\frac{\Delta E\, r}{c}\right]dr, \tag{6}$$

$$J^{(L)}=\int_0^\infty(P_\alpha P_\beta+Q_\alpha Q_\beta)j_L\left[\frac{\Delta E\, r}{c}\right]dr. \tag{7}$$

We also have the selection rules (Eq. 4.22 of Grant[20])

$$|j_\alpha-L|\le j_\beta\le j_\alpha+L$$

and

$$j_\alpha+j_\beta+L=\begin{cases}\text{odd} & \text{if } \kappa_\alpha\kappa_\beta>0\\ \text{even} & \text{if } \kappa_\alpha\kappa_\beta<0\end{cases}$$

(electric multipoles only).

For the electric dipole case ($L=1$), these formulas have been evaluated for Li $1s^2 2s \rightarrow 1s^2 2p$ and the Be I $1s^2 2s^2\ ^1S \rightarrow 1s^2 2s 2p\ ^1P$ transitions at the DF level. Comparison was made with the nonrelativistic case both formally (keeping only the first term in the small-r expansion of the spherical Bessel functions) and numerically. In all cases, the agreement was excellent.

B. Nonorthonormality

Because the many-electron wave functions are individually optimized, the one-electron functions from different states are not orthonormal. In earlier work,[23] we showed that the neglect of nonorthonormality (NON) can lead to errors of 1–100% in neutral and light ionized species. NON effects on electric dipole oscillator strengths were first successfully treated by Westhaus and Sinanoglu[24] following the work of King *et al.*[25] This method originally required two diagonalizations of matrices of the order of N (N denotes the number of electrons) for each pair of determinants. However, because the electric dipole operator involves a symmetry change [e.g., α and β in Eq. (3) do not have the same symmetry], it is possible[6,7] to avoid the diagonalization step entirely, speeding up calculation times by a *factor of 1000.* Computational costs of correctly evaluating NON effects are then nearly negligible.

Following the structure of our nonrelativistic electric dipole code,[6] we developed[26] a relativistic analog, RFE. The main differences are the following.

(i) A one-electron symmetry element is now specified by κ and m in place of l, m_l, and m_s.

(ii) The radial routines were replaced with ones to evaluate the I and J integrals. A one-electron subroutine from Desclaux's program[12] was used to do this, once it was modified to accommodate spherical Bessel functions.

C. FOTOS

First-order theory of oscillator strengths[11] (FOTOS) serve as a means to determine which are the most important classes of configurations present in the first-order RCI function, from the standpoint of the oscillator strength.

It is perhaps easiest to present FOTOS nonrelativistically, and then specialize it to the relativistic case. First, for each state, the major configurations are identified [those in the zeroth-order function, and perhaps one or two of the most important (weights >0.2) correlation configurations]. Each of these major configurations is reduced to a "pseudoconfiguration," in which only the occupation number of each symmetry (s,p,d,f, etc.) is counted (at this stage one normally makes the decision as to which subshells constitute the inactive core). The symmetry part of the dipole operator (the length form is easiest; i.e., $\hat{r}$), is then applied to these, to generate the pseudoconfigurations of the other state. These are then converted back to actual configurations (one can take NON effects into account at this stage).

It is perhaps useful to contrast some of the formal aspects of FOTOS with the random-phase approximation[27] (RPA) at this point. First, FOTOS excites from both states, not just the ground state as the RPA does. Secondly, FOTOS applies to all states, not just closed-shell ground states, as the RPA does. Thirdly, nonorthonormality effects are easily treated by FOTOS, unlike in the RPA. Finally one notes that for the RPA the length and velocity forms of the oscillator strength yield identical results.

Let us illustrate the FOTOS process for the transition of interest here. Suppose we allow the ground state to be represented by $5d^{10}(6s^2+6p^2)$ for FOTOS purposes; for the upper state we shall take $5d^{10}6s6p$ as the FOTOS starting point. The process and the final pseudoconfigurations required are shown in Table II. If we chose to completely neglect NON effects, FOTOS predicts that we must include $5d^{10}(6s^2+6p^2+6svs+6pvp)$ and $5d^9 6s(6p^2+6pvf+6pvp)$ in the lower state, and $5d^{10}(6s6p+6pvd+6svp)$ and $5d^9[6s^2(6p+vf+vp)+6p^2(6p+vf+vp)]$ in the upper state. All these configurations are significant; those with vf subshells are crucial to obtaining an accurate f value.

Relativistically, the only modifications needed are to replace each nonrelativistic configuration with all relativistic equivalents. These could be further screened by im-

TABLE II. Illustration of how to apply FOTOS.

Initial configuration (state 1)	Pseudoconfiguration	Result of applying $\hat{r}$	Conversion to actual configuration[a] (state 2)
$5d^{10}6s^2$	$d^{10}s^2$	$d^{10}sp$	$5d^{10}6sp$ $(p=6p,vp)$
$5d^{10}6s^2$	$d^{10}s^2$	d^9s^2p	$5d^96s^2p$ $(p=6p,vp)$
$5d^{10}6s^2$	$d^{10}s^2$	d^9s^2f	$5d^96s^2vf$
$5d^{10}6p^2$	$d^{10}p^2$	$d^{10}pd$	$5d^{10}6pvf$
$5d^{10}6p^2$	$d^{10}p^2$	d^9p^3	$5d^96p^2p$ $(p=6p,vp)$
$5d^{10}6p^2$	$d^{10}p^2$	d^9p^2f	$5d^96p^2vf$
$5d^{10}6s6p$	$d^{10}sp$	$d^{10}s^2$	$5d^{10}6ss$ $(s=6s,vs)$
$5d^{10}6s6p$	$d^{10}sp$	$d^{10}p^2$	$5d^{10}6pp$ $(p=6p,vp)$
$5d^{10}6s6p$	$d^{10}sp$	d^9sp^2	$5d^96s6pp$ $(p=6p,vp)$
$5d^{10}6s6p$	$d^{10}sp$	d^9spf	$5d^96s6pvf$

[a]Neglects NON effects.

posing the relativistic restriction $|j_\alpha - 1| \leq j_\beta \leq j_\alpha + 1$, although it is doubtful this will eliminate many configurations.

Since FOTOS is entirely based on angular-momentum considerations, decisions that must be based on the radial parts of the one-electron functions are left to the CI process itself. In addition to the question of what role NON will play, the questions which remain include the following. (1) What other configurations must be included, so that the CI coefficients and virtual functions of the FOTOS configurations are described properly? (2) What constitutes the core, i.e., what occupied subshells can we leave unexcited? Previous nonrelativistic work (e.g., Ref. 6) on oscillator strengths for nonshell jumping transitions (e.g., $6s \rightarrow 6p$; on the other hand, $6s \rightarrow 7p$ is a shell-jump transition) suggests as an answer to (1) that one need include *at most* those configurations arising from exciting the same shells as were excited to create the FOTOS configuration. For example, $5d^{10}6pvd$ created by exciting $6s$ to vd is, at most, coupled to all single and double excitations out of $6s, 6p$. As a second example, $5d^9 6s 6pvf$ arising from exciting $5d6s$ to $6pvf$ would at most involve all single and double excitations from $5l$, $6s$ ($l=0,1,2$).

While FOTOS concentrates exclusively on the transition matrix element, oscillator strengths also involve the excitation energy. It is well known that energy differences emphasize different, and generally harder to obtain, aspects of the wave function than do oscillator strengths. Our approach for f values has been, and remains, that when experimental energy differences are available, we use them, i.e., we do not complicate our calculations computing something well known. Although the *theoretical* energy differences which are a by-product of FOTOS calculations for oscillator strengths are not always in excellent agreement with experiment (generally, we do not report them), the combination of an experimental energy difference and a FOTOS calculation for the transition matrix element is *consistently* in good agreement with experimental f values, when they are available. Finally, this division of labor not only makes good computational sense, but it reflects the experimental situation—good-quality excitation energies are frequently available (if they are not, we have the capacity to compute them accurately—the calculations are simply substantially lengthened) whereas good-quality f values are relatively rare, particularly for the larger atomic species.

IV. APPLICATION

From our initial application, we chose a system which is simple (not many open subshells), that exhibits substantial relativistic and many-body effects, and is of technological importance. Our choice was to work on the Tl^+ $6s^2\,{}^1S_0 \rightarrow 6s6p\,{}^{1,3}P_1$ transitions; Tl^+'s importance is that, e.g., it serves as a substitutional impurity in NaI crystals, which are used in scintillation detectors. Except for the *ab initio* (MCDF) and semiempirical work of Migdalek and Baylis,[28] there has been no theoretical work on this transition; experimentally,[29] the "allowed" transition has been measured by the beam-foil method.

We begin by calculating the MCDF f values for the ${}^1S \rightarrow {}^1P$ transition; included in the lower state is the configuration $6s^2$ and for the upper $6s_{1/2}6p_{1/2}$ and $6s_{1/2}6p_{3/2}$ configurations. From Table III, we see that the length value is in particularly poor agreement with

TABLE III. Absorption oscillator strengths for Tl^+ $6s^2 \rightarrow 6s6p$.

Transition	Calculation type[a]	Excitation[b] energy (a.u.) Expt.	Theor.	Length	Velocity	Comments[c]
${}^1S_0 \rightarrow {}^1P_1$	MCDF	0.3446	0.3320	2.479	1.519	this work: NON
	MCDF	0.3446	0.3320	2.4993	1.532	this work: no NON
	MCDF+Corr. (6^2)	0.3446	0.3342	2.302	2.090	this work: NON
	MCDF+Corr. (6^2+5d6l)	0.3446	0.3811	1.3621	1.2487	this work: NON
	MCDF+Corr. (6^2+5d6l)	0.3446	0.3811	1.562	0.692	this work: no NON
	MCDF+polar			1.359		Ref. 28
	Experiment			1.21±0.20		Ref. 29
	NR HF (=RHF)	0.2556		2.8842	1.557	this work: NON
	RHF+Corr. (6^2)	0.2556		1.979	0.197	this work: NON
	RHF+Corr. (6^2+5d6l)	0.2556		1.830	1.375	this work: NON
	RHF+Corr. (6^2+56)	0.2556		1.818	1.438	this work: NON
${}^1S \rightarrow {}^3P_1$	MCDF	0.2386	0.1901	0.0561	0.0181	this work: NON
	MCDF+Corr. (6^2+5d6l)	0.2386	0.2727	0.0222	0.0115	this work: NON
	MCDF+polar			0.0449		

[a]MCDF denotes relativistic, multiconfigurational Dirac-Fock. Corr. (6^2) denotes first-order correlation involving $6s^2+6s6p$ excitations. Corr.($5d6l$) denotes first-order correlation involving $5d6l$ excitations. Corr.(5,6) denotes first-order correlation involving all $5l6l'$ excitations. RHF denotes nonrelativistic (NR) Hartree-Fock. Polar denotes core-polarization effects, treated semiempirically.

[b]The experimental value is from (Ref. 30); the theoretical value is from this work. When available, the experimental number was used to calculate the f value.

[c]NON denotes that effects of nonorthonormality are included.

experiment, and the effects of NON are small. In our calculations we turn NON off by setting all overlaps whose magnitude is >0.8 to 1.0 (maintaining the sign), and all those below 0.45 to 0.0 (none fall in the intermediate region). None of our wave functions were obtained in the presence of the Breit operator.

Next, we correlated the $n=6$ electron; for $6s^2$, we used $6s_{1/2}vs_{1/2}$, $vs^2_{1/2}$, $vp^2_{1/2}$, $vp^2_{3/2}$, $vd^2_{3/2}$, and $vd^2_{5/2}$; for $6s6p$ we used $s_{1/2}p_{1/2}$, $s_{1/2}p_{3/2}$, $p_{1/2}d_{3/2}$, $p_{3/2}d_{5/2}$, where $s=6s,vs$; $p=6p,vp$. The virtual basis sets were represented by screened hydrogenic functions (prior to orthogonalization) which were optimized during the RCI process. The final virtual basis sets are shown in Table IV. The optimization process was carried out as follows. We first represented each virtual basis set with a single screened hydrogenic function, and varied both the exponent (Z^* denotes the effective Z) and principle quantum number n (integer only) such that the CI energy was minimized. As expected,[5,6] the best parameter combinations n,Z^* were those giving the same average r as the spinors being removed ($6s,6p$). We did find that the lowest values of n ($n=1$ for s, $n=2$ for p, etc.) gave the lowest minimum. The nonrelativistic CI results provided an excellent guide to the relative sizes of the contributions of individual configurations. The f values were then calculated with this set. Next, we added a second screened hydrogenic function for each virtual, optimized them, and recalculated the f value, finding little change (e.g., 10% for the M shell, NON, allowed transition). From Table III, we see the main effect (NON on) of the $6s^2$ correlation is to raise the velocity value (further away from experiment).

In the final relativistic calculation for this transition, the $5d6l$ configurations which FOTOS requires (Table II) were included. The effect (NON on) is to bring the length and velocity results into dramatic agreement with experiment. On the other hand, turning NON off destroys the velocity value, and changes the length value substantially.

For the $^1S\rightarrow{}^3P_1$ transition, we show (Table III) the results of two relativistic calculations, both with NON on. We can see that the MCDF value is again dramatically changed by the inclusion of correlation effects (the same configurations were included for the $^3P_1$ as for the $^1P_1$). Now, however, the length and velocity results are not in very good agreement; this is not too surprising as a great deal of cancellation occurs for this transition (about 2 orders of magnitude). Clearly, more work (larger virtual and configurational basis sets) should be done.

As for the first transition, NON has little effect on the MCDF result, but a dramatic effect on the correlated f value. For comparison we show the results of a calculation by Migdalek and Baylis;[28] there is no experimental result.

All the relativistic f values reported here used experimental energy differences[30] for the reasons put forward earlier. In Table III, we also report the (unused) theoretical energy differences, which in the case of the CI results do not contain differential Breit contributions. As might be expected (no variational principle for energy differences, no direct attempt made to produce accurate energy differences), there is no pattern of convergence as more correlation (selected to optimize the description of the transition matrix elements) is added.

Also shown in Table III are some nonrelativistic results for the allowed f value. Obviously, no experimental nonrelativistic result exists—but such theoretical results may be of some use to us in directing the still novel relativistic calculations. The first question which arises is how do we get a nonrelativistic excitation energy without doing a prohibitive number of calculations. The crudest approximation (which was actually used) is to do a nonrelativistic RHF calculation for the excitation energy using the program of Froese-Fisher[31] and subtract it from the MCDF excitation energy, to get an approximate value for the relativistic contribution to this quantity. This is then subtracted from the experimental excitation energy,[30] to yield a nonrelativistic energy. The main correction to this estimate will be associated with the changing average radius of the outermost electrons, which will

TABLE IV. Radial parts of one-electron virtual functions used for Tl^+ f-value calculations. These are relativistic screened hydrogenic functions with principal quantum number n and effective charge Z^*.

	Tl^+ $6s^2$		Tl^+ $6s6p\,^1P^\circ_1$		Tl^+ $6s6p\,^3P^\circ_1$	
Type	n	Z^*	n	Z^*	n	Z^*
$s_{1/2}$	1	0.578	1	0.540	1	0.540
$p_{1/2}$	2	2.218	2	3.11	2	3.11
	3	7.0486	3	4.094	3	5.00
$p_{3/2}$	2	2.218	2	3.110	2	3.110
	3	7.0486	3	4.094	3	4.613
$d_{3/2}$	3	9.692	3	4.24	3	3.717
$d_{5/3}$	3	9.692	3	4.24	3	3.472
$f_{5/2}$	4	12.1055	4	7.920	4	7.92
			4	11.755	4	10.433
$f_{7/2}$	4	12.1055	4	7.920	4	7.92
			4	10.746	4	11.955

influence the differential $6l6l'$ and, to a lesser extent, $6l5l'$ correlation; for example, in the ground state the $6s$ electron has an average nonrelativistic radius of 2.8 a.u., whereas, relativistically, its value is 2.47 a.u. However, these corrections will enter only as overall scale factors—they will not affect the relative weight of each configuration in the f value.

As can be seen from Table III, the nonrelativistic velocity value is very sensitive to $6l6l'$ and $5d6l$ correlation, whereas the nonrelativistic length value is sensitive mainly to just $6l6l'$ correlation. All first-order configurations were used, but only the FOTOS ones contributed substantially to the f value. Finally, we examined $5s6l$ and $5p6l$ correlation; based on the average value of r ($5s$ versus $5p$ versus $5d$) there is no reason to exclude excitations from these subshells. Yet, little contribution to the f value occurred; closer examination showed that all FOTOS configurations, like $5p6s \rightarrow 6pvd$ involved vs, vp, or vd virtuals—no vf was present. But vs, vp, and vd virtual basis sets, unlike vf, are orthogonalized to $n=5$ occupied functions ($5s, 5p, 5d$) and this dramatically reduces the one-electron radial transition integrals (e.g., $\langle 5d|r|5p \rangle$ is twice as large as $\langle vd|r|5p \rangle$); moreover, the configurational coefficients are smaller for $5s6l$ and $5p6l$ excitations than for $5d6l$ excitations. The combination of these two factors serves to reduce contributions from the $5s$ and $5p$ subshells to a level where they do not need to be included (at least for $^1S \rightarrow {}^1P$).

There are two older calculations[15,32] on the $^1S \rightarrow {}^1P_1$ transition for Hg I which might be usefully contrasted to the present methodology and result. While each represented a significant contribution at the time they appeared, the methodologies employed and results obtained are not as complete as those appearing in this work.

The work of Desclaux and Kim[15] involved separate MCDF calculations for each state—in the lower state, configurations, nonrelativistically equivalent to $5d^{10}(6s^2 + 6p^2)$ and $5d^8 6s^2 6p^2$, were used; in the upper state, $5d^{10}6s6p$ and $5d^9 6s^2 6p$. The length value was found to be 1.53 compared to the experimental value[33] of 1.18. This was a striking improvement over both the nonrelativistic Hartree-Fock value (3.03) and the DF value (1.99), although the result was still about 30% in error. The key differences with the present approach lie in the absence of important core configurations (which FOTOS identifies), the absence of a treatment of nonorthonormality (although our work shows this has a small effect on the length value for the types of configurations they used), and the absence of an independent velocity result, which can be used as a negative check on one's results.

Earlier in the text, we have contrasted the current methodology with that of the RPA. In comparing to the RPA work of Shorer[32] on Hg I, the following points are of interest. (1) There is a significant cancellation of the errors in the excitation energy and transition matrix element leading to a nearly errorless (1.10 and 1.15) result for the f value. But there is no guarantee this will happen consistently. To be specific, there is an 11% error in the theoretical energy difference; if the experimental energy difference is used, a length value of 1.24 and a velocity value of 1.03 is obtained for the f value. (2) As is characteristic of the RPA method, no excitations are made from the upper state, so that some important configurations are missing. Although it is hard to make further observations with any assurance, due to the absence of details, we might summarize this work as representing an improvement over the earlier work[15] in that it includes important core excitations from the ground state not previously considered.

ACKNOWLEDGMENTS

The authors gratefully acknowledge the financial support of the U.S. National Science Foundation Grant No. PHY-87-15246.

[1]D. R. Beck, Z. Cai, and G. Aspromallis, Int. J. Quantum Chem. Symp. **21**, 457 (1987).
[2]D. R. Beck, Phys. Rev. A **37**, 1847 (1988).
[3]D. R. Beck and Z. Cai, Phys. Rev. A **37**, 4481 (1988).
[4]D. R. Beck and C. A. Nicolaides, Int. J. Quantum Chem. Symp. **8**, 17 (1974); **10**, 119 (1976).
[5]D. R. Beck and C. A. Nicolaides, in *Excited States in Quantum Chemistry,* edited by C. A. Nicolaides and D. R. Beck (Reidel, Dordrecht, 1978), p. 105.
[6]C. A. Nicolaides and D. R. Beck, in *Excited States in Quantum Chemistry,* edited by C. A. Nicolaides and D. R. Beck (Reidel, Dordrecht, 1978), p. 143.
[7]D. R. Beck, Phys. Rev. A **23**, 159 (1981).
[8]C. A. Nicolaides, Phys. Rev. A **6**, 2078 (1972).
[9]See, e.g., *Relativistic Effects in Atoms, Molecules, and Solids,* edited by G. L. Malli (Plenum, New York, 1981).
[10]See, e.g., Y. Ishikawa, Chem. Phys. Lett. **101**, 111 (1983); R. E. Stanton and S. Havriliak, J. Chem. Phys. **81**, 1910 (1984).
[11]C. A. Nicolaides and D. R. Beck, Chem. Phys. Lett. **36**, 79 (1975).
[12]J. P. Desclaux, Comput. Phys. Commun. **9**, 31 (1975).
[13]D. R. Beck, program RELRED (unpublished).
[14]I. Oksuz and O. Sinanoglu, Phys. Rev. **181**, 42 (1969).
[15]H. F. Schaefer, R. A. Klemm, and F. E. Harris, Phys. Rev. **181**, 137 (1969).
[16]C. F. Bunge, Phys. Rev. A **14**, 1965 (1976).
[17]Based on formal theory appearing in D. R. Beck, J. Chem. Phys. **51**, 2171 (1969).
[18]J. P. Desclaux and Y. K. Kim, J. Phys. B **8**, 1177 (1975).
[19]D. R. Beck *et al.*, Phys. Rev. A **28**, 2634 (1983).
[20]I. P. Grant, J. Phys. B **7**, 1458 (1974).
[21]A. R. Edmonds, *Angular Momentum in Quantum Mechanics* (Princeton University Press, Princeton, NJ, 1960).
[22]F. A. Babushkin, Opt. Spectrosc. (USSR) **13**, 77 (1962).
[23]C. A. Nicolaides and D. R. Beck, Can. J. Phys. **53**, 1224 (1975).
[24]P. Westhaus and O. Sinanoglu, Phys. Rev. **183**, 56 (1969).
[25]H. F. King *et al.*, J. Chem. Phys. **47**, 1936 (1967).
[26]D. R. Beck, program RFE (unpublished).
[27]See, e.g., W. R. Johnson and C. D. Lin, Phys. Rev. **14**, 1965

(1976).
[28]J. Migdalek and W. E. Baylis, J. Phys. B **18**, 1533 (1985).
[29]T. Andersen, A. K. Nielsen, and G. Sorenson, Phys. Scr. **6**, 122 (1972).
[30]C. E. Moore, *Atomic Energy Levels,* Nat. Bur. Stand. (U.S.) Circ. No. 467 (U.S. GPO, Washington, D.C., 1958), Vol. 3.
[31]C. Froese-Fisher, Comput. Phys. Commun. **4**, 107 (1972).
[32]P. Shorer, Phys. Rev. A **24**, 667 (1981).
[33]A. Lurio, Phys. Rev. **140**, A1505 (1965).